BUILDING STRUCTURES, BUILDINGS AND CONSTRUCTIONS

DOI 10.36622/VSTU.2021.51.3.001
UDC 624.012.45

N. I. Karpenko[1], Vl. I. Kolchunov[2], V. I. Travush[3]

CALCULATION MODEL OF A COMPLEX STRESS REINFORCED CONCRETE ELEMENT OF A BOXED SECTION DURING TORSION WITH BENDING

Research Institute of Structural Physics (NIISF) [1, 2, 3]
Russia, Moscow
Southwestern State University (SWU) [2]
Russia, Kursk

[1]*D. Sc. in Engineering, Prof., Head of Lab., RAASN Academician, e-mail: niisf_lab9@mail.ru*
[2]*D. Sc. in Engineering, Prof., Prof. of the Dept. of Unique Buildings and Structures, Major Researcher, RAASN Academician, e-mail: vlik52@mail.ru*
[3]*D. Sc. in Engineering, Prof., Major Researcher, RAASN Academician, e-mail: travush@mail.ru*

Statement of the problem. Based on the analysis of domestic and foreign scientific publications and guidelines, it is found that the known deformation models for the calculation of complex tensile reinforced concrete elements during torsional bending are quite conditional. Therefore the article considers the solution of the problem of designing a computational model of a reinforced concrete element during torsion with bending in the post-crack stage, which most fully accounts for the specifics of crack formation, deformation and destruction of such elements. The case is considered for when among all possible external influences the action of torques and bending moments has the greatest influence on the stress-strain.

Results. Using the equations of statics and physical ratios of reinforced concrete, the calculated parameters are identified such as stresses in concrete of compressed zone, height of compressed concrete, stresses in clamps, deformations in concrete and reinforcement, curvature and torsion angle of reinforced concrete element.

Conclusions. The obtained analytical dependences were tested by means of numerical calculation of the reinforced concrete strapping crossbar of the outer contour of a residential building of box section of high-strength concrete. The suggested deformation model can be employed in the design of a wide class of reinforced concrete structures working on torsional bending.

Keywords: reinforced concrete, design model, deformation, complex resistance, torsion with bending, cracks.

Introduction. Despite reinforced concrete structures undergoing a complex stress state — torsion with bending being relatively common in the practice of design and construction, methods for calculating the strength of such structures examined in scientific publications (e.g., [1, 9, 16, 17], etc.) and those used in the guidelines of different countries are not sufficiently rigorous. So, outdated models of the girder analogy are still in use in the EU regulations.

In the domestic guidelines and regulations of the CIS countries, the section method is traditionally employed, which is very conditional when applied to the complex stress. Besides, in the above studies, the solution of problems of strength in bending with torsion is mainly discussed. A model for calculating the angles of twisting and curvatures in reinforced concrete elements in bending with torsion (deformation model) was set forth in [4—6]. In this case, an approach was used with the selection of the design contour of the cross section which is intersected by a spiral crack or its part. A more general model of the mechanics of cracked reinforced concrete in a volumetric stress was presented in the fundamental monograph [8]. Finite element models are currently increasingly used in studies of the complex resistance of reinforced concrete structures. They make it possible to obtain acceptable solutions while calculating in a linearly elastic formulation, as well as in a nonlinear formulation when the given physical-mechanical and stiffness characteristics are used. At the same time, according to experimental [2, 3, 12—14, 19] and numerical studies [9, 10, 18], physical modeling of the crack formation process itself is required based on the general methodology for solving the problem of rigidity, crack resistance and strength of reinforced concrete [11, 18], and the development of the design scheme itself by considering a number of new effects of deformation. This is what makes the study timely and relevant.

The aim of the work is to design a compact and, at the same time, a more general design model of a complexly stressed reinforced concrete box-section element experiencing the combined action of bending M and torque T moments in the stage after the formation of spatial cracks considering the shape of the cross-section, the spatial nature of the cracks, the stress state in longitudinal and transverse rods, as well as in the concrete of the compressed zone.

1. Design model of a complex stressed reinforced concrete moment. In order to design a computational model, the approach [6, 7] is used with the allocation of the computational contour of the most stressed spatial cross-section.

The cross-section of a box-shaped element with section $h \times b$ is reinforced with two longitudinal reinforcement bars in a tensioned zone with a total area of $2F_s$ and in a compression zone with a total area of $2F_{s'}$. The distance between the rods is h_1 and b_1 (Fig. 1b). The transverse reinforcement is bordered by closed clamps with the area of the rods F_{sw} and the pitch U_{sw0}, h_1 and b_1 are the dimensions of the clamps.

In the design model, the clamps are transferred to the level of longitudinal reinforcement (Fig. 1b) with a reduced pitch U_{sw}, where

$$U_{sw} = U_{sw0} \frac{(b_1 + h_1)}{(b_2 + h_2)}. \quad (1)$$

The reduced running area of the clamps will be

$$F_{sw} = F_{sw} / U_w = F_{sw} \frac{(b_2 + h_2)}{(b_1 + h_1) U_{sw0}}. \quad (2)$$

Fig. 1 shows two cases.

In the first case, this is the height of the compressed zone:

$$X_T = 2a', \quad (3)$$

where a' is the distance from the upper surface of the section to the center of gravity of the reinforcement in the compressed zone. In this case, the section height is taken equal to h_1.

In the second case $XT > 2a'$, with the height being taken equal to Z_1.

Let us look at a more general second case.

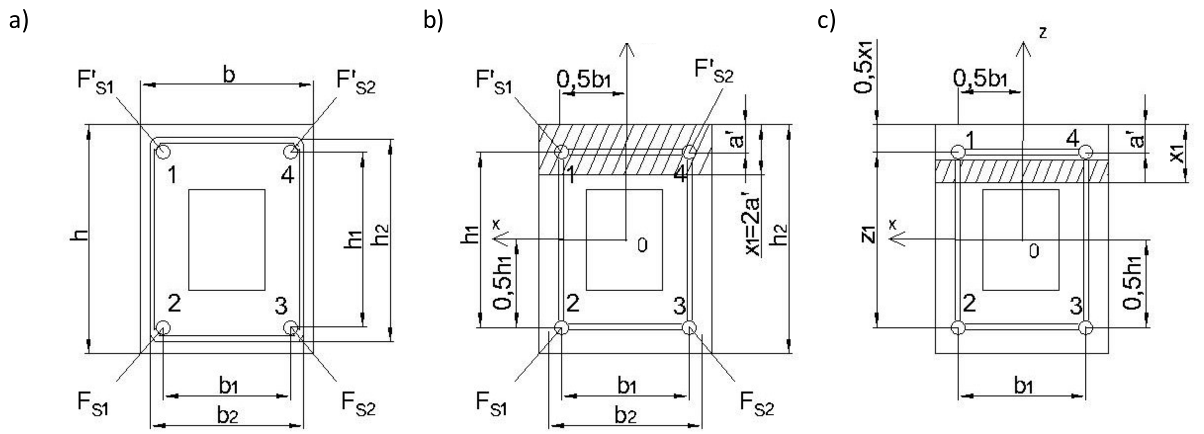

Fig. 1. Cross-sectional box diagram (a)
with the allocation of calculated contours 1—2—3—4 (b) according to a particular scheme,
(c) — according to the general scheme

2. Identifying the shear force flows. The transition to the first case is performed by replacing Z_1 with h_1. Let us select from the box-shaped section the calculated box-shaped element of size $b_1 \times Z_1$ (Fig. 2) where Z_1 is the distance from the tensioned reinforcement $2F_s$ to the center of gravity of the concrete in the compressed zone

$$Z_1 = h_1 + a' - 0.5X_T. \quad (4)$$

In this case, the reinforcement of the compressed zone is transferred to the new line 1—4 to the safety margin. Also, the linear reduced area of the clamps is somewhat specified

$$f_{sw} = F_{sw}\frac{(b_1+h_1)}{(b_1+Z_1)U_{sw0}}. \quad (5)$$

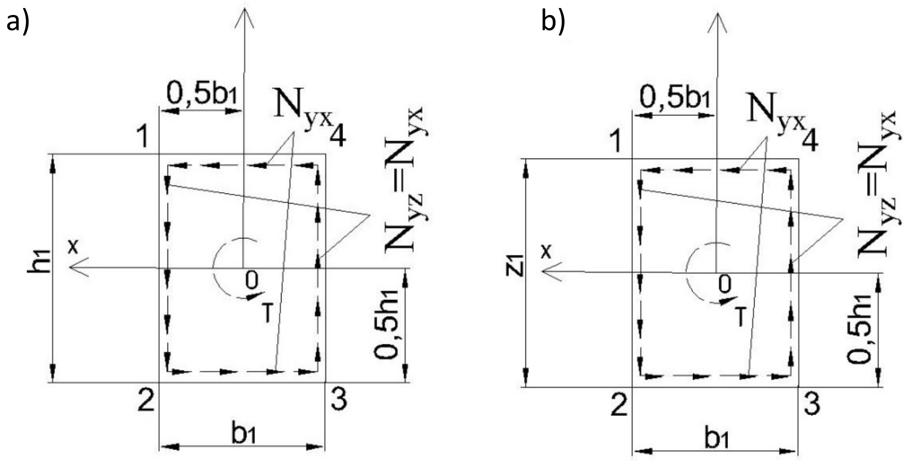

Fig. 2. Scheme of shear force flows N_{yx}, N_{zy} from the action of the torque according to the calculated contours 1—2—3—4, (a) — according to a particular scheme, (b) — according to the general scheme

The action of the torque is reduced to the action of the flow of tangential forces N_{yx} and N_{zy} along the contour 1—2—3—4 in the general case (Fig. 2b):

$$N_{yx} = N_{yz} = \frac{T}{2(b_1+Z_1)}. \quad (6)$$

Here below the general case is discussed. In a particular case in all the formulas, Z_1 is replaced by h_1.

The design diagram of the box-shaped element is shown in Fig. 3. On the left side, the design scheme is limited by the design rectangular contour 1—2—3—4. M — bending moment, T — torque are applied to a rectangular contour centered at point 0.

The action of the torque T on the contour of the element 1—2—3—4 is represented in the form of flows N_{yz} (1), N_{yz} (2), N_{yx}. The total flow of tangential forces along the line 1—2 will be:

$$N_{yz(1)} = N_{yz} = \frac{T}{2(b_1+z_1)}. \quad (7)$$

A similar flow of tangential forces along line 3—4 will be equal to:

$$N_{yz(2)} = N_{yz} = \frac{T}{2(b_1+z_1)}. \quad (8)$$

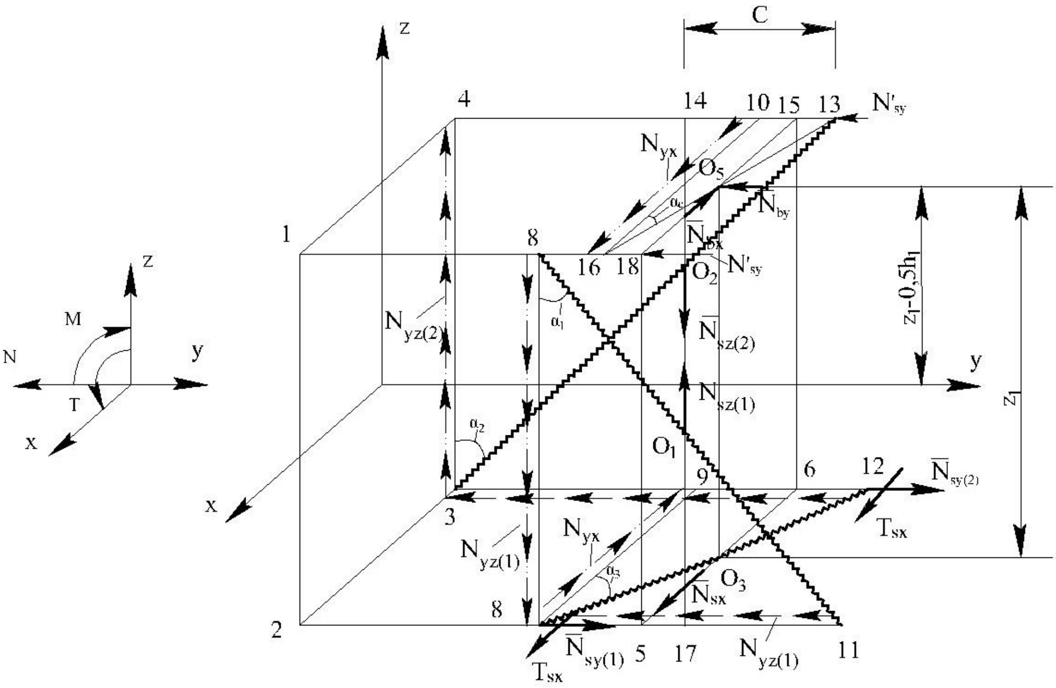

Fig. 3. Design diagram of a box-shaped element

On the left side, the contour is limited with the lines 7—11, 11—8, 8—12, 12—3, 3—13, 13—16, 16—7.

3. Efforts and stresses in the concrete of the compressed zone along a line lying in the plane of the upper face of the design element. A sloped line 13—16 represents that of the application of the main compressive effort $\overline{N}_b$ in the concrete of the compressed zone.

Fig. 3 shows the projections $\overline{N}_{bx}$ $\overline{N}_{by}$ of this effort on the *x*, *y* axis, applied to the midpoint of the line 13—16 (at point 0_c), the main compressive effort will be equal to:

$$\overline{N}_b = \overline{N}_{by} \cos a_c + \overline{N}_{bx} \sin \alpha_c, \quad (9)$$

where ac is the inclination angle of the line of the compressed zone 13—16 to the line 7—10 parallel to the axis *x*. This angle is identified based on the equality to zero by the projection $\overline{N}_{by}$ and $\overline{N}_{bx}$ onto the sloped line 13—16, $\overline{N}_{bx} \cos \alpha_c - \overline{N}_{by} \sin \alpha_c = 0$, hence

$$\operatorname{tg} \alpha_c = \frac{\overline{N}_{bx}}{\overline{N}_{by}}. \quad (10)$$

The main stresses in the concrete of the compressed zone with a rectangular diagram will be equal to:

$$\sigma'_b = -\frac{\overline{N}_b}{F_c}, \quad (11)$$

where Fc is the area of the concrete of the compressed zone which is identified considering the entire section of the element:

$$F_c = X_T b / \cos \alpha_c , \tag{12}$$

where b is the width of the section (see Fig. 1).

4. Identifying stresses in closed transverse clamps. Sloped lines 7—11 and 3—13 run along inclined cracks; $\bar{N}_{sz(1)}$, $\bar{N}_{sz(2)}$ are the total forces applied to clamps that cross oblique cracks. These forces are identified based on the flows of shear forces $N_{yz}(1)$, $N_{yz}(2)$ (formulas (7) and (8)) applied to the lines 7—8 and 3—4. As a result,

$$\left.\begin{aligned} \bar{N}_{sz(1)} &= N_{yz(1)} Z_1 = \frac{TZ_1}{2(b_1 + Z_1)}, \\ \bar{N}_{sz(2)} &= N_{yz(2)} Z_1 = \frac{TZ_1}{2(b_1 + Z_1)}. \end{aligned}\right\} \tag{13}$$

The efforts $\bar{N}_{sz(1)}$ and $\bar{N}_{sz(2)}$ are also expressed in terms of stresses (respectively σ_{sz} (1) and σ_{sz} (2)) in vertical clamps based on the dependencies:

$$\left.\begin{aligned} \sigma_{sz(1)} f_{sw} l_{8-11} &= \sigma_{sz(1)} f_{sw} Z_1 \operatorname{tg} \alpha_1 = \bar{N}_{sz(1)}, \\ \sigma_{sz(2)} f_{sw} l_{4-13} &= \sigma_{sz(2)} f_{sw} Z_1 \operatorname{tg} \alpha_2 = \bar{N}_{sz(2)}. \end{aligned}\right\} \tag{14}$$

Using these ratios, considering (13), it is possible to identify the stresses in the vertical rebars of transverse reinforcement:

$$\left.\begin{aligned} \sigma_{sz(1)} &= \frac{T}{2(b_1 + Z_1) f_{sw} tg\alpha_1}, \\ \sigma_{sz(2)} &= \frac{T}{2(b_1 + Z_1) f_{sw} tg\alpha_2}. \end{aligned}\right\} \tag{15}$$

The common effort $\bar{N}_{sx}$ in clamps crossing an inclined crack 8—12, together with the thrust efforts applied to the longitudinal reinforcement, will be

$$\bar{N}_{sx} + 2T_{sx} = N_{yx} l_{8\text{-}9} = N_{yx} b_1. \tag{16}$$

In this case, the thrust efforts in the clamps are not considered — only the thrust forces T_{sx} in the longitudinal reinforcement are. According to [6, 7], the influence of the thrust forces can be taken into account using the coefficient λ_x.

Wherein

$$\bar{N}_{sx} = N_{yx1} b_1 - 2T_{sx} \approx N_{yx} b_1 \lambda_x , \tag{17}$$

where

$$\lambda_x = \frac{15 f_{sw}}{15 f_{sw} + f_{sy} \operatorname{ctg}^2 \alpha_3}, \tag{18}$$

where

$$f_{sy} = \frac{2F_{sy}}{b_1}. \tag{19}$$

The effort $\overline{N}_{sx}$ can be expressed using the stresses σ_{sx} in the lower clamps:

$$\overline{N}_{sx} = N_{yx} b_1 \lambda_x = \sigma_{sx} f_{sw} b_1 \operatorname{tg} \alpha_3, \tag{20}$$

hence

$$\sigma_{sx} = \frac{N_{yx} \lambda_x}{f_{sw} tg \alpha_3} = T \frac{\lambda_x}{2(b_1 + Z_1) f_{sw} tg \alpha_3}. \tag{21}$$

5. Identifying the efforts in the concrete of the compressed zone. The projection of all efforts applied to the right calculated curvilinear contour on the x axis leads to the dependence

$$\overline{N}_{bx} - \overline{N}_{sx} + 2T_{sx} = \overline{N}_{bx} - N_{yx} b_1 = 0.$$

Hence, given (5):

$$\overline{N}_{bx} = N_{yx} b_1 = \frac{T b_1}{2(b_1 + Z_1)}. \tag{22}$$

Let us move on to identifying $\overline{N}_{by}$. Let us denote:

$$\overline{N}'_y = \overline{N}_{by} + N'_{sy}. \tag{23}$$

The sum of the moments of all forces acting parallel to the plane $Z0Y$ relative to the lower line parallel to b_1 and passing through the lower point O_3 will be:

$$\overline{N}'_y \times Z_1 + \overline{N}_{sz(1)} l_{5\text{-}17} + \overline{N}_{sz(2)} l_{14\text{-}15} + N_{yx} l_{7\text{-}16} \times Z_1 - M = 0, \tag{24}$$

where $M = M_e$, M_e is the moment at the point e in the line y (Fig. 4).

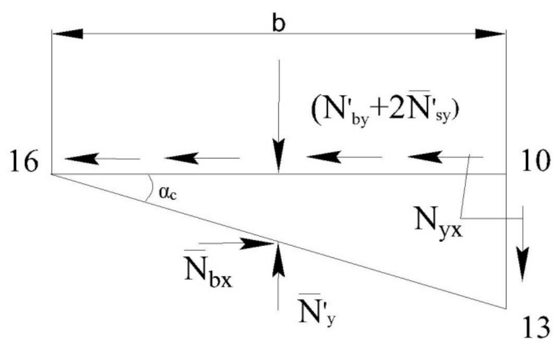

Fig. 4. Typical calculation element of the compressed concrete zone

According to Fig. 2,

$$\left.\begin{aligned} l_{5\text{-}17} &= 0.5Z_1 \operatorname{tg}\alpha_1 - 0.5b_1 \operatorname{tg}\alpha_3, \\ l_{14\text{-}15} &= 0.5Z_1 \operatorname{tg}\alpha_2 - 0.5b_1 \operatorname{tg}\alpha_c, \\ l_{19\text{-}0c} &= Z_1 \operatorname{tg}\alpha_2 - 0.5b_1 \operatorname{tg}\alpha_c, \\ l_{7\text{-}16} &= 0.5b_1\left(\operatorname{tg}\alpha_3 - \operatorname{tg}\alpha_c\right). \end{aligned}\right\} \tag{25}$$

Based on these values, according to (22) and (24),

$$\bar{N}'_y = \frac{M_e}{Z_1} - \frac{\bar{N}_{sz(1)}\left(Z_1 \operatorname{tg}\alpha_1 - b_1 \operatorname{tg}\alpha_3\right)}{2Z_1} - \frac{\bar{N}_{sz(2)}\left(Z_1 \operatorname{tg}\alpha_2 - b_1 \operatorname{tg}\alpha_c\right)}{2Z_1} - 0{,}5N_{yx}b_1(\operatorname{tg}\alpha_3 - \operatorname{tg}\alpha_c). \tag{26}$$

Considering the dependencies (13), formula (26) is transformed as follows:

$$\begin{gathered} \bar{N}'_y = \bar{N}_{by} = \frac{M_e}{Z_1} - \left(\frac{T}{4(b_1 + Z_1)}\right)\left(Z_1 \operatorname{tg}\alpha_1 - b_1 \operatorname{tg}\alpha_c\right) - \\ -\left(\frac{T}{4(b_1 + Z_1)}\right)\left(Z_1 \operatorname{tg}\alpha_2 - b_1 \operatorname{tg}\alpha_c\right) - \frac{Tb_1(\operatorname{tg}\alpha_3 - b_1 \operatorname{tg}\alpha_c)}{4(b_1 + Z_1)}. \end{gathered} \tag{27}$$

Let us isolate from the general scheme shown in Fig. 3 the element of the compressed zone 16—10—13 with an effort applied to it: ($N'_{by} + 2N'_{sy}$) are the normal efforts in concrete and two transverse rods of the compressed zone, N_{yx} are tangential efforts; $\bar{N}_{bx}$ and $\bar{N}_y$ are the efforts along the sloped line 16—13. The projection of the efforts of the element16—10—13 onto the y' axis is (Fig. 4):

$$\bar{N}'_y - N_{yx}b \operatorname{tg}\alpha_c = N'_{by} + 2N'_{sy}; \tag{28}$$

or

$$\bar{N}'_y - N_{yx}b \operatorname{tg}\alpha_c = \sigma'_{by}bX_t + 2\sigma'_{sy}F'_s, \tag{29}$$

where σ'_{by}, σ'_{sy} are the normal stresses in concrete and reinforcement on the verge of 16—10; X_t is the height of the compressed concrete zone.

Let us denote ε'_y as the deformations of the element along the y' axis. Based on the condition of the joint deformation of the concrete and reinforcement,

$$\varepsilon'_y = \frac{\sigma'_{by}}{\nu'_b E_b} = \frac{\sigma'_{sy}}{E_s}, \tag{30}$$

where E_b, E_s are the modules of the deformation of the concrete and reinforcement; ν'_b is the secant modulus of concrete ($\nu'_b \approx 0.75$). Thus

$$\sigma'_{by} = \sigma'_{sy}\frac{\nu'_b E_b}{E_s} = \beta'_b \sigma'_{sy} \quad , \tag{31}$$

where

$$\beta'_b = \frac{\nu'_b E_b}{E_s}, \tag{32}$$

Inserting (31) into (29) leads to the dependence:

$$\sigma'_{sy} = (\bar{N}'_y - N_{xy}\ \mathrm{tg}\,\alpha_c)\big/\left(\beta'_b b X_T + 2F'_s\right), \tag{33}$$

hence

$$2N'_{sy} = \frac{2\bar{N}'_y F'_s}{\left(\beta'_b b X_T + 2F'_s\right)} - \frac{2N_{xy} b\,\mathrm{tg}\,\alpha \bar{N}'_y F'_s}{\left(\beta'_b b X_T + 2F'_s\right)}. \tag{34}$$

Let us denote:

$$c_1 = \frac{2F'_s}{\left(\beta'_b b X_T + 2F'_s\right)};\quad c_x = c_1 b. \tag{35}$$

As a result, the dependence (33) is written as

$$2N'_{sy} = \bar{N}'_y c_1 - 2N_{xy} b c_1\ \mathrm{tg}\,\alpha_c. \tag{36}$$

Let us denote the value $\bar{N}_{by}$ considering (23) and (36):

$$\begin{gathered}\bar{N}_{by} = \frac{M_e(1-c_1)}{Z_1} - \left(\frac{T}{4(b_1+Z_1)}\right)(Z_1\ \mathrm{tg}\,\alpha_1 - b_1\ \mathrm{tg}\,\alpha_3)(1-c_1) - \\ -\left(\frac{T}{4(b_1+Z_1)}\right)(Z_1\ \mathrm{tg}\,\alpha_2 - b_1\ \mathrm{tg}\,\alpha_c)(1-c_1) + \frac{Tb_1}{4(b_1+Z_1)}\left[(1+3c_1)\,\mathrm{tg}\,\alpha_c - (1-c_1)\,\mathrm{tg}\,\alpha_3\right]\end{gathered} \tag{37}$$

Entering the values $\bar{N}_{by}$ and $\bar{N}_{bx}$ into the dependence (10) given by the formulas (37), (22), we move to a quadratic equation for tgαc:

$$\begin{gathered}\frac{M_e(1-c_1)}{Z_1} - \left(\frac{T}{4(b_1+Z_1)}\right)(Z_1 tg\alpha_1 - b_1 tg\alpha_c)(1-c_1) + \\ +\left(\frac{T}{4(b_1+Z_1)}\right) b_1(\mathrm{tg}\,\alpha_3\ \mathrm{tg}\,\alpha_c)(1-c_1) - \left(\frac{T}{4(b_1+Z_1)}\right) Z_1(\mathrm{tg}\,\alpha_3\ \mathrm{tg}\,\alpha_c)(1-c_1) + \\ +\left(\frac{T}{4(b_1+Z_1)}\right) b_1(\mathrm{tg}\,\alpha_c{}^2)(1-c_1) + \left(\frac{T}{4(b_1+Z_1)}\right) b_1(\mathrm{tg}\,\alpha_c{}^2)(1-3c_1) - \\ -\left(\frac{T}{4(b_1+Z_1)}\right) b_1(\mathrm{tg}\,\alpha_3\ \mathrm{tg}\,\alpha_c)(1-c_1) - \left(\frac{Tb_1}{2(b_1+Z_1)}\right) = 0.\end{gathered} \tag{38}$$

Therefore the angle αc is identified using the solution of the quadratic equation (27) with respect to the unknown tgα_c. In the first approximation, depending on (36), (37), we can take α_2 = 450:

$$\alpha_1 \approx \alpha_2 N_{yz(1)} / N_{yz(2)}. \tag{39}$$

The maximum compressive stresses in concrete σ_b' are given by the formulas (11)—(12):

$$\sigma_b' = -\frac{\bar{N}_b \cos\alpha_c}{bX_T}. \tag{40}$$

In the specific stage $\sigma_b' = R_b$, considering the effect of the compressed reinforcement as a result the specific height $X_T = \hat{X}_T$ will be:

$$\hat{X}_T = \frac{\left(\bar{N}_b - 2F_s' R_{sc}\right)\cos\alpha_c}{R_b b}. \tag{41}$$

6. Identifying the height of the compressed concrete zone and the shoulder of the internal pair of forces in the design section. In order to identify the height of the compressed zone X_T and the shoulder of the internal pair of forces in the design section Z_1 and in the operational stage, the formula of SP (СП) 63.13330.2018 can be used with some approximation.

For this, the following needs to be identified:

– additional section characteristics:

$$\left.\begin{aligned} h_0 &= 0.5\left(h_1 + h\right), \\ h_f' &= \left(h_1 - h\right); \end{aligned}\right\} \tag{42}$$

– given moment:

$$\begin{aligned} \bar{M} &= M_e + N_{yx} \cdot l_{3\text{-}12} \cdot Z_1 + N_{yz(1)} \cdot l_{8\text{-}11} \cdot Z_1 - \bar{N}_{sz(1)} \cdot l_{5\text{-}17} - \bar{N}_{sz(2)} \cdot l_{14\text{-}15} = \\ &= M_e + \frac{TZ_1'}{2\left(b_1 + Z_1\right)}\left[Z_1 \operatorname{tg}\alpha_2 + 0.5b_1\left(\operatorname{tg}\alpha_3 - \operatorname{tg}\alpha_c\right)\right] + \left(\frac{T}{2\left(b_1 + Z_1\right)}\right) \cdot Z_1^2 \operatorname{tg}\alpha_1 - \\ &- \left(\frac{TZ_1}{2\left(b_1 + Z_1\right)}\right) \cdot 0.5\left(Z_1 \operatorname{tg}\alpha_1 - b_1 \operatorname{tg}\alpha_3\right) - \left(\frac{TZ_1}{2\left(b_1 + Z_1\right)}\right) \times \\ &\times 0.5\left(Z_1 \operatorname{tg}\alpha_2 - b_1 \operatorname{tg}\alpha_c\right) = M_e + \frac{TZ_1}{2\left(b_1 + Z_1\right)} \cdot \left(0.5Z_1 \operatorname{tg}\alpha_2 + 0.5Z_1 \operatorname{tg}\alpha_1 + b_1 \operatorname{tg}\alpha_3\right); \end{aligned} \tag{43}$$

– given normal force $\bar{N}$:

$$\begin{aligned} \bar{N} &= N_{yx}\left(l_{3-12} + l_{7-16}\right)_1 + N_{yz(1)} Z_1 \operatorname{tg}\alpha_1 = \\ &= \frac{T}{2\left(b_1 + Z_1\right)}\left[Z_1 \operatorname{tg}\alpha_2 + b_1\left(\operatorname{tg}\alpha_3 - \operatorname{tg}\alpha_c\right)\right] + \frac{T}{2\left(b_1 + Z_1\right)} Z_1 \operatorname{tg}\alpha_1 = \\ &= \frac{T}{2\left(b_1 + Z_1\right)}\left[Z_1\left(\operatorname{tg}\alpha_1 + \operatorname{tg}\alpha_2\right) + b_1\left(\operatorname{tg}\alpha_3 - \operatorname{tg}\alpha_c\right)\right]. \end{aligned} \tag{44}$$

In practical calculations, in dependences (41), (42), it is allowed to take $Z_1 = h_1$. In this case, as shown below, after identifying Q_b according to the procedure indicated below, Z_1 can be set and this value can be used while determining the remaining values.

Following SP (СП) 63.13330.2018, the relative height of the compressed zone is given by the formula

$$\xi = \left(\frac{1}{\beta + \frac{1 + 5(\delta + \lambda)}{10\mu\alpha}} \right), \tag{45}$$

where β is the coefficient considering the type and class of concrete accepted in compliance with SP (СП) 63.13330.2018:

$$\begin{gathered} \delta = \frac{\bar{M}}{bh_0^2 R_{b,\,ser}};\ \lambda = f_f \times \left(1 - \frac{h_f'}{2h_0}\right);\ f_f = \frac{\alpha A_s' / 2\nu}{bh_0} 9;\ \nu = 0.45;\ \alpha = \frac{E_s}{E_b};\ \mu = \frac{A_s}{A_{red}}; \\ \delta = \frac{\bar{M}}{bh_0^2 R_{b,\,ser}};\ \lambda = \phi_f \cdot \left(1 - \frac{h_f'}{2h_0}\right);\ \phi_f = \frac{\alpha A_s' / 2\nu}{bh_0} 9;\ \nu = 0.45;\ \alpha = \frac{E_s}{E_b};\ \mu = \frac{A_s}{A_{red}}, \end{gathered} \tag{46}$$

A_s' is the total area of the reinforcement of the compressed area $(A_s' = 2F_s')$.

The value Z1 is given by the formula:

$$Z_1 = h_0 \left[1 - \frac{\frac{h_f'}{h_0} f_f + \xi^2}{2(f_f + \xi)} \right]. \tag{47}$$

The height of the compressed zone is

$$X_T = 2(h_0 - Z_1). \tag{48}$$

In this case, considering the dependences (11), (12), the main compressive stresses in line 16—13 will be

$$\sigma_b' = -\frac{\bar{N}_b \cos\alpha_c}{X_T b}. \tag{49}$$

7. Identifying the forces and stresses in tensile reinforcement bars. By projecting all the forces applied to the design element (see Fig. 3) along the y axis onto the horizontal plane, there is direct consideration of the forces $N'_{sx(1)}$ and $N'_{sy(2)}$ in the reinforcement of the compressed zone to the dependence:

$$\begin{gathered} N'_{sy(1)} + N'_{sy(2)} = \\ = N_y' + N_{yx}\left[Z_1 \operatorname{tg}\alpha_2 + b_1\left(\operatorname{tg}\alpha_3 - \operatorname{tg}\alpha_c\right)\right] + N_{yz(1)} Z_1 \operatorname{tg}\alpha_1. \end{gathered} \tag{50}$$

The rotation of the forces around the O_c–O_3 axis in the plane *yZ* without any consideration of the forces $N'_{sx(1)}$, $N'_{sy(2)}$ either leads to the equation:

$$N'_{sy(2)}l_{0_3\text{-}6} + T_{sx}l_{6\text{-}12} + N_{yz(1)}Z_1 \operatorname{tg}\alpha_1 l_{0_3\text{-}5} - T_{sx}l_{8\text{-}5} - \bar{N}_{sy(1)}l_{0_3\text{-}5} - 0.5N_{yx}b_1 Z_1 \operatorname{tg}\alpha_2 = 0. \quad (51)$$

Given that

$$\left.\begin{aligned} l_{0_3-6} &= l_{0_3-5} = 0.5b_1, \\ l_{6-12} &= l_{8-5} = 0.5b_1 \operatorname{tg}\alpha_3, \end{aligned}\right\} \quad (52)$$

the equation (51) is transformed as follows:

$$\bar{N}_{sy(2)} - \bar{N}_{sy(1)} = N_{yx}Z_1 \operatorname{tg}\alpha_2 - N_{yz(1)}Z_1 \operatorname{tg}\alpha_1. \quad (53)$$

The joint solution of the equations (50), (53) in relation to $\bar{N}_{sx(1)}$ and $\bar{N}_{sy}$ leads to the dependencies:

$$\begin{aligned} \bar{N}_{sy(1)} &= 0.5\bar{N}'_y + N_{yz(1)}Z_1 \operatorname{tg}\alpha_1 + 0.5N_{yx}b_1\left(\operatorname{tg}\alpha_3 - \operatorname{tg}\alpha_c\right), \\ \bar{N}_{sy(2)} &= 0.5\bar{N}'_y + N_{yx}\left[Z_1 \operatorname{tg}\alpha_2 + 0.5b_1\left(\operatorname{tg}\alpha_3 - \operatorname{tg}\alpha_c\right)\right]. \end{aligned} \quad (54)$$

According to the dependencies (54), the tensile stresses in the lower longitudinal reinforcement bars F_{s1} and F_{s2} will differ slightly. They align in areas where the shear force Q is zero, which corresponds to the case of bending with torsion. However, for the sake of generality, the formulas $\bar{N}_{sy(1)}$ and $\bar{N}_{sy(2)}$ are retained.

The stresses in the lower reinforcement rods of will be:

$$\left.\begin{aligned} \sigma_{sy(1)} &= \frac{\bar{N}_{sy(1)}}{F_{sy(1)}} = \frac{0.5\bar{N}'_y + N_{yz(1)}Z_1 tg\alpha_1 + 0.5N_{yx}b_1\left(tg\alpha_3\text{-}tg\alpha_c\right)}{F_{sy(1)}}, \\ \sigma_{sy(2)} &= \frac{\bar{N}_{sy(2)}}{F_{sy(2)}} = \frac{0.5\bar{N}'_y + N_{yx}\left[Z_1 tg\alpha_2 + 0.5b_1\left(tg\alpha_3\text{-}tg\alpha_c\right)\right]}{F_{sy(2)}}. \end{aligned}\right\} \quad (55)$$

Identifying the deformations in the lower zone of the element (conventionally in the zone 2—3). Relative deformations in bars 1 and 2 of the lower longitudinal reinforcement are given by the dependencies:

$$\varepsilon_{sy(1)} = \frac{\sigma_{sy(1)}\Psi_{sy(1)}}{E_s}; \ \varepsilon_{sy(2)} = \frac{\sigma_{sy(2)}\Psi_{sy(2)}}{E_s}, \quad (56)$$

where $\Psi_{sy}(1)$, $\Psi_{sy}(2)$ are the coefficients that consider the effect of adhesion of reinforcement to concrete in the areas between cracks (V. I. Murashev's coefficients):

$$\Psi_{sy(1)} = 1 - 0,75\phi_{sl}\frac{\sigma_{crc}}{\sigma_{sy(1)}}; \quad \Psi_{sy(2)} = 1 - 0,75\phi_{sl}\frac{\sigma_{crc}}{\sigma_{sy(2)}}, \quad (57)$$

where σ_{cr} are the stresses in the reinforcement at the time of cracking, which in a first approximation can be given by the formula:

$$\sigma_{crc} \approx \frac{2.5R_{btsen}E_s}{E_b}, \quad (58)$$

$\phi_{sl} = 1$ under a one-time load, $\phi_{sl} = 0.8$ under a long-term load.

The average deformations of the reinforcement are

$$\varepsilon_{sy} = \frac{\varepsilon_{sy(1)} + \varepsilon_{sy(2)}}{2}. \quad (59)$$

The average deformations of the lower clamp rods are

$$\varepsilon_{sx} = \frac{\sigma_{sx}\psi_{sx}}{E_s};$$
$$\psi_{sx} = 1 - 0,75\phi si\frac{\sigma_{crc}}{\sigma_{sx}}. \quad (60)$$

After there have been cracks of stress σbt and deformations ε_{bt} of the concrete strips along the cracks will mainly depend on the tangential stresses τ_{yx}:

$$\left.\begin{aligned} \sigma_{bt} &\approx -2\tau_{yx}\sin\alpha_3\cos\alpha_3, \\ \varepsilon_{bt} &\approx \frac{\sigma_{bt}}{E_{П}\nu_{nx}} = -\frac{2\tau_{yx}\sin\alpha_3\cos\alpha_3}{E_{П}\nu_{nx}}, \end{aligned}\right\} \quad (61)$$

where $E_{П}$ is the modulus of deformation of the concrete strips:

$$E_{П} = E_b\beta_{П} \approx 0.8E_b, \quad (62)$$

$\beta_{П} \approx 0.8$ is the coefficient of influence of loosening of concrete strips by cracks on the module; ν_{nx} is the coefficient considering the effect of plastic deformations of concrete strips in the process of increasing stresses ε_{bt}.

Shear stresses are identified as a function of linear shear forces N_{yx}:

$$\tau_{yx} \approx \frac{N_{yx}}{2a\beta_{xy}}, \quad \sigma_{bt} = -\frac{2N_{yx}\sin\alpha_3\cos\alpha_3}{2a\beta_{xy}}, \quad (63)$$

where α is the thickness of the protective layer of the lower reinforcement; β_{xy} is the coefficient of the influence of the remaining concrete layers on τ_{yx}; the minus sign means that the strips are compressed.

Given (62), (63):

$$\varepsilon_{bt} = -\frac{2N_{yx}\sin\alpha_3\cos\alpha_3}{2\alpha\beta_{xy}E_b\beta_{П}\nu_{Пx}} = -\frac{2N_{yx}\sin\alpha_3\cos\alpha_3}{2\alpha E_b\tilde{\nu}_{Пx}}, \quad (64)$$

where

$$\tilde{\nu}_{Пx} = \beta_{П}\nu_{Пx}\beta_{xy}. \quad (65)$$

The coefficient $\tilde{\nu}_{\Pi x}$ is identified experimentally and $\nu_{\Pi x}$ can be given by the formula shown below (68). According to [6, 7] and given (64), the shear angle in the lower zone 2—3 will be:

$$\gamma_{xy} = \varepsilon_{sx} ctg\alpha_3 + \varepsilon_{sy} tg\alpha_3 - \varepsilon_{bt} / \sin\alpha_3 \cos\alpha_3 = \frac{\sigma_{sx}\Psi_{sx}}{E_s} ctg\alpha_3 + \frac{\sigma_{sy}\Psi_{sy}}{E_s} tg\alpha_3 + \frac{2N_{xy}}{2aE_b\tilde{\nu}_{\Pi x}}, \quad (66)$$

where E_s is the modulus of reinforcement deformation in the plastic stage of reinforcement deformation, everywhere Es is replaced by $E_{s}\nu_{s}$, where νs is the secant modulus given by the dependencies [8].

8. Identifying the deformations in the upper compression zone of concrete. The deformation of concrete in the compressed zone is given by the dependence:

$$\varepsilon'_b = \frac{\sigma'_b}{E_b \nu'_b} = \frac{N'_b}{F_c E_b \nu'_b}, \quad (67)$$

where F_c is the area of the concrete of the compressed zone given by the formula (12); ν'_b is the coefficient of the development of plastic deformations in the concrete of the compressed zone. Based on [8], the coefficient ν'_b is given by the formula:

$$\nu'_b = \hat{\nu}'_b \pm \left(\nu_0 - \hat{\nu}'_b\right)\sqrt{1 - \omega\eta' - (1-\omega)(\eta')^2} \quad (68)$$

(for the ascending branch of the diagram, the sign <+> is taken, and for the descending branch, the sign <–>), where

— the level of the main stresses in concrete (positive value) where η' is the level of the main stresses in concrete (positive value):

$$\eta' = \frac{\sigma'_b}{\hat{\sigma}'_b}, \quad (69)$$

where the current main stresses σ'_b given by the formula (11); $\hat{\sigma}'_b$ are the stresses at the top of the diagram $\left(\hat{\sigma}'_b = -R_{b,ser}\right)$; $\hat{\nu}'_b$ is the coefficient of change of the secant modulus at the top of the diagram (positive value):

$$\hat{\nu}'_b = \frac{\hat{\sigma}'_b}{E_b \hat{\varepsilon}'_b}, \quad (70)$$

$$\hat{\varepsilon}'_b = -\frac{B}{E_b}\lambda \frac{1 + \left(0.8 - 0.15\frac{B^2}{10000}\lambda B/60 + 0.2\lambda/B\right)}{0.12 + 1.03B/60}, \quad (71)$$

here B is the concrete class corresponding to Rb ser; λ is the dimensionless coefficient depending on the concrete type (for heavy and fine-grained concrete λ = 1); vb is the initial coefficient of change of the secant module; ω is the coefficient characterizing the curvature of the diagram.

For the ascending branch of the diagram depending on (71):

$$\nu_0 = 1; \quad \omega = 2 - 2.5\hat{\nu}'_{b1}; \tag{72}$$

for the descending branch of the diagram:

$$\nu_0 = 2.05\hat{\nu}'_b, \quad \omega = 1.95\hat{\nu}'_b - 0.138. \tag{73}$$

The above formulas refer to the case of compression of the upper concrete zone (zones 1—4) at $\sigma'_b < 0$. In case the main stresses are tensile ones $(\sigma'_b = \sigma'_{bt} > 0)$, but there have not been any cracks yet, the diagram of concrete tensile $(\varepsilon'_{bt} - \sigma'_{bt})$ should be given by the formulas (58)—(64) where где ε'_b, $\hat{\varepsilon}'_b$, σ'_b, $\hat{\sigma}'_b$, ν'_b, $\hat{\nu}'_b$, $\hat{\nu}'_b$ are replaced by ε'_{bt}, $\hat{\varepsilon}'_{bt}$, σ'_{bt}, $\hat{\sigma}'_{bt}$, ν'_{bt}, $\hat{\nu}'_{bt}$, η'_t respectively:

$$\eta'_t = \sigma'_{bt} / \hat{\sigma}'_{bt}, \tag{74}$$

where $\hat{\sigma}'_{bt}$, $\hat{\varepsilon}'_{bt}$ are the stresses and relative deformations at the top of the tensile diagram for the normative diagram:

$$\hat{\sigma}'_{bt} = R_{bt.ser}\gamma_{btq}; \quad \hat{\varepsilon}_{bt} = \frac{\hat{\sigma}'_{bt}}{E_b \hat{\nu}_{bt}}, \tag{75}$$

where

$$\hat{\nu}'_{bt} = \left(0.55 + 0.15R_{bt.ser} / R_{0bt}\right) / \tilde{\gamma}_{btq}. \tag{76}$$

Here R_{bt} = 2.5 MPa; γ_{btq} is the coefficient considering the influence of the deformation gradients for crack resistance:

$$\tilde{\gamma}_{btq} = \left(\tilde{\gamma}_b + 0.007\right). \tag{77}$$

Here $0.9 \le \tilde{\gamma}_b = 2 - \sqrt[5]{h/h_э}$, $h_э = 0.3$ m is some exemplary height (the values $\tilde{\gamma}_{btq}$ were identified for the bending elements, for the torsion bending a specification $\tilde{\gamma}_{btq}$ might be needed.

The normal σ'_{by} and tangential τ'_{xy} stresses in the cocnrete of the compressed zone acting normally and along the line 7—10 (Fig. 4) will be:

$$\sigma'_{by} = -\frac{\left(\bar{N}_{by} - N_{yc}b_1 tg\alpha_c\right)}{F'_{cy}} = -\frac{\bar{N}_{by} - N_{yx}b_1 tg\alpha_c}{X_T b}; \tau'_{xy} = \frac{N_{yx}}{X_T}. \tag{78}$$

Accordingly, the normal and shear relative deformations will be:

$$\varepsilon'_{by} = \frac{\sigma'_{by}}{E_b \nu'_b} = -\frac{\left(\bar{N}_{by} - N_{yx}b_1 tg\alpha_c\right)}{X_T b E_b \nu'_b}, \quad \gamma'_{xy} = -\frac{2N_{yx}\left(1 + \mu'_b\right)}{X_T E_b \nu'_b}, \tag{79}$$

where μ_b' is the coefficient of the transverse deformations of the concrete.

$$\mu_b' = \hat{\mu}_b' + \left(\mu_b - \hat{\mu}_b'\right)\sqrt{1-\eta'}\,; \tag{80}$$

μ_b is the initial coefficient of the transverse deformations of the concrete $\left(\mu_b \approx 0.175\right)$; $\hat{\mu}_b'$ is the coefficient corresponding to the top of the diagram:

$$\hat{\mu}_b' = \mu_b + \left(1 - \sqrt[3]{\hat{\nu}_b'}\right); \tag{81}$$

$\bar{N}_{by}$ is given by the formula (35) and N_{yx} by the formula (6). The curvature of the element and relative deformations ε_{0y} at the level of the y axis.

After identifying ε_{sy} using the formula (59) and ε_{by}' using the formula (79) , the curvature of the element and the relative deformations ε_{0y} can be identified:

$$\left.\begin{aligned} \frac{1}{\rho_y} &= \frac{\varepsilon_{sy} - \varepsilon_{by}'}{Z_1}, \\ \varepsilon_{0y} &= \frac{\varepsilon_{sy}\left(Z_1 - 0.h_1\right) + 0.5\varepsilon_{by}' h_1}{Z_1}. \end{aligned}\right\} \tag{82}$$

Expressing ε_{sy} and ε_{by}' using the common efforts M, T based on the formulas (59) and (79), we will get the ultimate dependencies for identifying the curvature of the relative deformations ε_{0y}.

9. Shear angles of the vertical walls of the element. Let us consider the element 7—8—11 (Fig. 3, 4). The average relative deformations of this element along the axis y will be:

$$\varepsilon_{y(1)} = \frac{\varepsilon_{sy(1)} + \varepsilon_{by}'}{2}, \tag{83}$$

where $\varepsilon_{sy}(1)$, ε_{by} are given by the formulas (56), (79).

The stresses $\sigma_{sy}(1)$ in the vertical rods of the clamps are

$$\sigma_{sz(1)} = \frac{\bar{N}_{sz(1)}}{f_{sw} Z_1 tg\alpha_1}. \tag{84}$$

Accordingly, the relative deformations of the vertical rods of the stirrups in the range 7—8—9 will be:

$$\varepsilon_{sz(1)} = \varepsilon_{sz(2)} = \frac{\sigma_{sz(1)}\Psi_{sz(1)}}{E_s}, \tag{85}$$

where

$$\Psi_{sz(1)} = \Psi_{sz(2)} = 1 - 0,75\phi_{sl}\frac{\sigma_{crc}}{\sigma_{sz(i)}};$$

$\Psi_{sz(1)}$ is given by the formula (57) where $\sigma_{sy(i)}$ is replaced by $\sigma_{sz(1)}$, in the plastic stage of the reinforcement deformation E_s is replaced by $E_s \nu_s$. The formulas (61) — (66) still hold true where τ_{xy} is replaced by τ_{Zy}, N_{yx} by $N_{Zy(1)}$, α_3 by α_1, in the indices x by $Z_{(1)}$. As a result,

$$\gamma_{yZ(1)} = \varepsilon_{sZ(1)} ctg\alpha_1 + \varepsilon'_{by} tg\alpha_1 + \frac{2N_{yZ(1)}}{2aE_b \tilde{\nu}_{nyZ(1)} - \tilde{\nu}_{\Pi Z(1)}}, \tag{86}$$

where similarly to the formula (65):

$$\left.\begin{aligned} &\tilde{\nu}_{\Pi Z(1)} = \beta_\Pi \nu_{\Pi Z(1)} \beta_{yZ(1)}, \\ &\beta_\Pi \approx 0.8, \quad \beta_{yZ(1)} \approx \beta_{xy}. \end{aligned}\right\} \tag{87}$$

Using the formula (15), we get the expression $\gamma_{yz(1)}$ into the function of T. Let us look at the element 3—4—13. The stresses $\sigma_{sZ(2)}$, deformations $\varepsilon_{Z(2)}$ and shear angles $\gamma_{yZ(2)}$ are given by the formulas (83) — (87), $\varepsilon_{y(1)}$, $\varepsilon_{sy(1)}$, $\sigma_{sz(1)}$, $\bar{N}_{sz(1)}$, α_1, $\Psi_{sz(1)}$, $\tilde{\nu}_{\Pi yZ(1)}$, $\beta_{\Pi yZ(1)}$, $\beta_{yZ(1)}$ are replaced by $\varepsilon_{y(2)}$, $\varepsilon_{sy(2)}$, $\sigma_{sz(2)}$, $\bar{N}_{sz(2)}$, α_2, $\Psi_{sz(2)}$, $\tilde{\nu}_{\Pi yZ(2)}$, $\beta_{\Pi yZ(1)}$, $\beta_{yZ(1)}$ respectively. As a result,

$$\left.\begin{aligned} &\varepsilon_{y(2)} = \frac{\varepsilon_{sy(2)} + \varepsilon'_{by}}{2}, \\ &\sigma_{sz(2)} = \frac{\bar{N}_{sz(2)}}{f_{sw} Z_1 tg\alpha_2}, \\ &\varepsilon_{sz(2)} = \frac{\sigma_{sz(2)} \Psi_{sz(2)}}{E_s}, \end{aligned}\right\} \tag{88}$$

$$\gamma_{yz(2)} = \varepsilon_{sz(2)} ctg\alpha_2 + \varepsilon_{y(2)} tg\alpha_2 + \frac{2N_{yz(2)}}{2aE_b \tilde{\nu}_{\Pi Z(2)}}, \tag{89}$$

where $\tilde{\nu}_{\Pi Z(2)} = \beta_\Pi \nu_{\Pi Z(2)} \beta_{yZ(2)}$, $\beta_\Pi \approx 0.8$, $\beta_{yZ(2)} \approx \beta_{xy}$. Based on the dependencies (15) the shear angle $\gamma_{yZ(2)}$ is expressed using the values T.

The torque angle ϕ, based on [6, 7] is identified using the values of the shear angles (γ_{xy} of the lower surface according to (66), γ'_{xy} of the upper compressed zone according to (79), $\gamma_{yZ(1)}$ of the first vertical wall according to (86) and $\gamma_{yZ(2)}$ of the second vertical wall according to (89)) according to the formula

$$\phi = \frac{b_1\left(\gamma_{xy} + \gamma'_{xy}\right) + Z_1\left(\gamma_{yZ(1)} + \gamma_{yZ(2)}\right)}{2b_1 Z_1}. \tag{90}$$

Based on the dependencies (6)—(8), (13), (15), (35), (55), (66) the torque angle ϕ is expressed in the function of M and T.

10. Additional remarks on the design of complex stressed reinforced concrete bars of solid cross-section in torsion with bending. The above dependences are designed so that the wall thickness of the element is not limited and makes it possible to switch to a solid section. It should only be noted that in elements of a solid section, according to [15], after the formation of cracks, part of the torque T_2 can be perceived by some still solid core of the section, which remains in the element following the cracking, and part of the moment T_1 is perceived by the section with a crack. Moreover, in the above formulas, T is replaced by T_1, according to the study by T. P. Chistova:

$$T = T_1 + T_2; \quad T_1 = T\left[1 - 0.3\left(\frac{T_{cr}}{T}\right)^4\right], \tag{91}$$

where T_{cr} is the torque moment at the moment of cracking; T is the current moment ($T > T$).

In bending with torsion, the effect of the concrete core in [15] should be taken into account only in the presence of spiral cracks developing along the entire contour. In the presence of concrete in the compressed zone without cracks, the effect of the concrete core can be neglected, assuming $T_2 = 0$.

Conclusions

1. An updated block design model of the complex resistance of reinforced concrete structures of a box section, experiencing the combined action of bending and torque moments after the formation of spatial cracks, which, on the one hand, is limited by a calculated rectangular contour, on the other hand, is a spatial surface with planes inclined to the edges of the structure, has been designed. The stresses in the concrete of the compressed zone and the height of the compressed concrete, the stresses in the clamps, the deformations in the compressed zone, in the rods of the longitudinal and transverse reinforcement, the curvature of the element and the angle of its twisting are identified using the equations of statics in the sections intersected by the faces of the spatial crack and element with cracks.

2. In the suggested design model, a variant is considered when out of three external influences: torque T, bending M moments, and transverse force Q during torsion with bending, the greatest influence on the stress-strain of the structure is exerted by the moments T and M. The moment is reduced to the action of the flow of tangential forces along a rectangular contour.

3. The suggested analytical model for calculating design parameters can be used in designing a wide class of reinforced concrete structures of buildings and structures from ordinary and

high-strength concrete and fiber-reinforced concrete under the considered complex stress in these structures.

References

1. Arzamastsev S. A., Rodevich V. V. K raschetu zhelezobetonnykh elementov na izgib s krucheniem [To the calculation of reinforced concrete elements for bending with torsion]. *Izvestiya vuzov. Stroitel'stvo*, 2015, no. 9, pp. 99—109.

2. Dem'yanov A. I., Sal'nikov A. S., Kolchunov Vl. I. Eksperimental'nye issledovaniya zhelezobetonnykh konstruktsii pri kruchenii s izgibom i analiz ikh rezul'tatov [Experimental studies of reinforced concrete structures under torsion with bending and analysis of their results]. *Stroitel'stvo i rekon-struktsiya*, 2017, no. 4 (72), pp. 17—26.

3. Dem'yanov A. I., Kolchunov Vl. I., Pokusaev A. A. Eksperimental'nye issledovaniya deformirovaniya zhelezobetonnykh konstruktsii pri kruchenii s izgibom [Experimental study of deformation of reinforced concrete structures in torsion with bending]. *Stroitel'naya mekhanika inzhener-nykh konstruktsii i sooruzhenii*, 2017, no. 6, pp. 37—44.

4. Karpenko N. I. [determination of the deformations of the core elements of reinforced concrete box cracked torsional]. *Referativnyi sb. TsINISA: Mezhotraslevye voprosy stroitel'-stva. «Otechestvennyi opyt»* [Abstract collection of TSINIS: Intersectoral issues of construction. "Domestic experience"], 1970, no. 10.

5. Karpenko N. I., Elagin E. G. Deformatsii zhelezobetonnykh trubchatykh elementov, podvergnutykh krucheniyu posle obrazovaniya treshchin [Deformation of reinforced concrete tubular members subjected to torsion after cracking]. *Beton i zhelezobeton*, 1970, no. 3, pp. 3—12.

6. Karpenko N. I. [To the calculation of deformation of reinforced concrete members with cracks under bending with torsion-received]. *Sb. NIIZhB: Teoriya zhelezobetona, posvyashchennom 75-letiyu so dnya rozhdeniya A. A. Gvozdeva* [Proc. NIIZHB: Theory of reinforced concrete, devoted to the 75 anniversary since the birth of A. A. Gvozdev]. Moscow, Stroiizdat Publ., 1972, pp. 50—59.

7. Karpenko N. I. *Teoriya deformirovaniya zhelezobetona s treshchinami* [The Theory of deformation of reinforced concrete with cracks]. Moscow, Stroiizdat Publ., 1976. 208 p.

8. Karpenko N. I. *Obshchie modeli mekhaniki zhelezobetona* [General models of reinforced concrete mechanics]. Moscow, Stroiizdat Publ., 1996. 410 p.

9. Kasaev D. Kh. Prochnost' betonnykh i treshchinostoikost' zhelezobetonnykh elementov pryamougol'nogo secheniya pri kruchenii i izgibe s krucheniem [Strength of concrete and crack resistance of reinforced concrete elements of rectangular cross-section during torsion and bending with torsion]. *Beton i zhelezobeton v tret'em tysyacheletii*, 2000, pp. 164—171.

10. Kolchunov V. I., Kolchunov Vl. I., Fedorova N. V. Deformatsionnye modeli zhelezobetona pri osobykh vozdeistviyakh [Deformation models of reinforced concrete under special influences]. *Promyshlennoe i grazhdanskoe stroitel'stvo*, 2018, no. 8, pp. 54—60.

11. Kolchunov Vl. I., Fedorov V. S. Ponyatiinaya ierarkhiya modelei v teorii soprotivleniya stroitel'nykh konstruk-tsii [Conceptual hierarchy of models in the theory of resistance of building structures]. *Promyshlennoe i grazhdanskoe stroitel'stvo*, 2020, no. 8, pp. 16—23. doi: 10.33622/0869-7019.2020.08.16-23.

12. Travush V. I., Karpenko N. I., Kolchunov V. I., Kaprielov S. S., Dem'yanov A. I., Konorev A. V. Rezul'taty eksperimental'nykh issledovanii konstruktsii kvadratnogo i korobchatogo sechenii iz vysokoprochnogo betona pri kruchenii s izgibom [The Results of experimental studies of the structures of square and box-like cross-sections of high-strength concrete in torsion with bending]. *Stroitel'stvo i rekonstruktsiya*, 2018, no. 6—80, pp. 32—43.

13. Travush V. I., Karpenko N. I., Kolchunov V. I., Kaprielov S. S., Dem'yanov A. I., Bulkin S. A., Moskovtseva V. S. Rezul'taty eksperimental'nykh issledovanii slozhnonapryazhennykh balok kruglogo poperechnogo secheniya iz vysokoprochnogo fibrozhelezobetona [Results of experimental studies of complex-stressed beams of circular cross-section made of high-strength fibro-reinforced concrete]. *Stroitel'naya mekhanika inzhenernykh konst-ruktsii i sooruzhenii*, 2020, no. 4, pp. 290—297.

14. Travush V. I., Karpenko N. I., Kolchunov V. I., Kaprielov S. S., Dem'yanov A. I., Konorev A. V. Osnovnye rezul'taty eksperimental'nykh issledovanii zhelezobetonnykh konstruk-tsii iz vysokoprochnogo betona V100 kruglogo i kol'tsevogo sechenii pri kruchenii s izgibom [The main results of experimental studies of reinforced concrete structures made of high-strength concrete B100 of round and annular sections during torsion with bending]. *Stroitel'naya mekhanika in-zhenernykh konstruktsii i sooruzhenii*, 2019, no. 1, pp. 51—61.

15. Chistova T. P. [Experimental study of deformations of ordinary reinforced concrete elements of box-shaped and solid rectangular cross-section under pure torsion]. *Prochnost' i zhest-kost' zhelezobetonnykh konstruktsii* [Strength and stiffness of reinforced concrete structures]. Moscow, Stroiizdat Publ., 1971.

16. Klein G., Lucier G., Rizkalla S., Zia P., Gleich H. Torsion simplified: a failure plane model for desigh of spandrel beams. *ACI Concrete International Journal*, 2012, pp. 1—19.

17. Kalkan I., Kartal S. Torsional Rigidities of Reinforced Concrete Beams Subjected to Elastic Lateral Torsional Buckling. *International Journal of Civil and Environmental Engineering*, 2017, no. 7, pp. 969—972.

18. Karpenko N. I., Kolchunov Vl. I., Kolchunov V. I., Travush V. I. Calculated model of a complex-stressed reinforced concrete element under torsion with bending. *International Journal for Computational Civil and Structural Engineering*, 2021, vol. 17, no. 1, pp. 34—47.

19. Travush V. I., Karpenko N. I., Kolchunov V. I., Kaprielov S. S., Demyanov A. I., Bulkin S. A., Moskovtseva V. S. Results of experimental studies of high-strength fiber reinforced concrete beams with round cross-sections under combined bending and torsion. Structural Mechanics of Engineering Constructions and Buildings, 2020, vol. 16, no. 4, pp. 290—297.